

Radiative properties of the first galaxies: Rapid transition from blue to red

Shohei Arata¹ , Hidenobu Yajima², Kentaro Nagamine^{1,3,4} ,
Yuxing Li⁵ and Sadegh Khochfar⁶

¹Theoretical Astrophysics, Department of Earth and Space Science, Graduate School of Science, Osaka University, Toyonaka, Osaka 560-0043, Japan
email: arata@astro-osaka.jp

²Center for Computational Sciences University of Tsukuba, Ibaraki 305-8577, Japan

³Department of Physics & Astronomy, University of Nevada, Las Vegas, 4505 S. Maryland Pkwy, Las Vegas, NV 89154-4002, USA

⁴Kavli IPMU (WPI), The University of Tokyo, 5-1-5 Kashiwanoha, Kashiwa, Chiba, 277-8583, Japan

⁵Department of Astronomy & Astrophysics, The Pennsylvania State University, 525 Davey Lab, University Park, PA 16802, USA

⁶SUPA, Institute for Astronomy, University of Edinburgh, Royal Observatory, Edinburgh, EH9 3HJ, UK

Abstract. Combining cosmological hydrodynamic simulations and radiative transfer (RT) calculations, we present predictions of multi-wavelength radiative properties of the first galaxies at $z \sim 6 - 15$. We find that intermittent star formation due to supernova (SN) feedback causes the escape fraction of UV photons to fluctuate rapidly, which then produces the observed diversity of SEDs for high- z galaxies. The simulated galaxies make rapid transition between UV-bright and IR-bright phase, and our RT calculations suggest that dust temperatures in the first galaxies are higher than $z < 3$ galaxies with ~ 60 K.

Keywords. galaxies: formation, galaxies: high-redshift, methods: numerical, radiative transfer

1. Introduction

Recent observations have successfully detected galaxies in the early Universe, the so-called *first galaxies*, in optical and near-infrared wavelengths (e.g. [Bouwens et al. 2015](#)), or in sub-millimeter wavelengths (e.g. [Hashimoto et al. 2018](#)). This variety of radiative properties probably reflects different physical conditions in the first galaxies, such as the escape fraction of ionizing and UV photons. Here we investigate the radiative output of first galaxies by applying RT calculations on zoom-in hydrodynamic simulations, as reported in [Arata et al. \(2018\)](#).

2. Method & Result

We use zoom-in cosmological hydrodynamic simulations from [Yajima et al. \(2017\)](#), which focused on massive galaxies and satellites with halo masses $1.6 \times 10^{11} h^{-1} M_\odot$ (Halo-11) and $0.7 \times 10^{12} h^{-1} M_\odot$ (Halo-12) at $z = 6$. We also use the multi-wavelength RT code ART² ([Li et al. 2008](#); [Yajima et al. 2012](#)), which computes the RT on an adaptive mesh refinement grid. The minimum spatial resolution is less than 10 pc at $z \sim 10$.

Figure 1 shows the redshift evolution of physical properties of Halo-11. At the end of their lifetime, massive stars explode as SNe and disrupt central star-forming gas clouds.

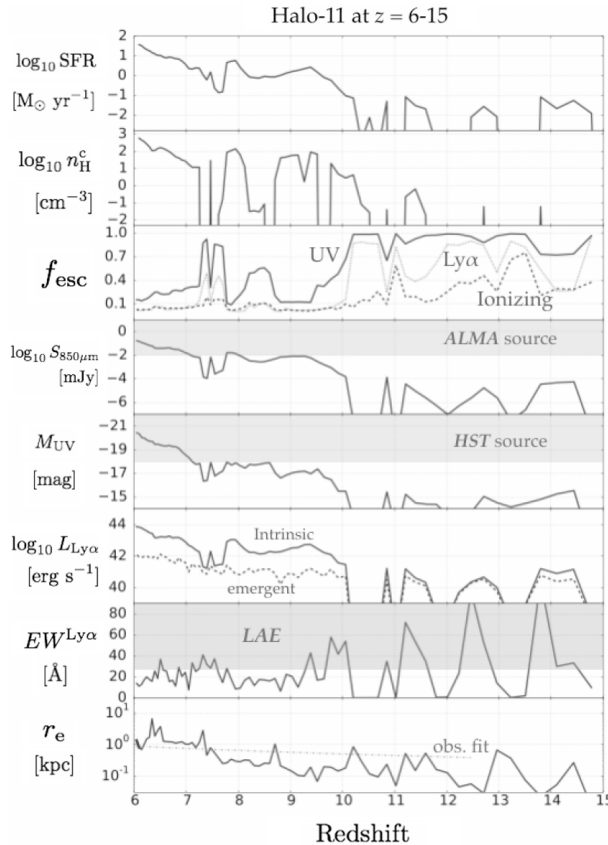


Figure 1. From top to bottom panels: Redshift evolution of SFR; central gas density; escape fraction of UV (solid), Ly α (dotted) and ionizing photons (dashed); observed-frame sub-millimeter flux; UV absolute magnitude; Ly α luminosity; Ly α equivalent width; and UV half-light radius of Halo-11 at $z = 6 - 15$. In the fourth (fifth) panel, shaded area represents the sensitivity of 10-hr observation by ALMA (HST). In the second bottom panel, the shaded region represents $EW^{\text{Ly}\alpha} > 30 \text{ \AA}$, which is often used as a criterion to define LAEs. In the bottom panel, the dashed line represents the observational fit by Kawamata *et al.* (2018), who used bright galaxies with $-21 < M_{\text{UV}} < -20.5$ mag. The size of simulated galaxy increases similarly to virial radius ($\propto M_{\text{h}}^{1/3} (1+z)^{-1}$) with decreasing redshift.

This results in intermittent star formation (see also Yajima *et al.* 2017). The UV photons escape more efficiently when the gas density becomes lower in galactic center. Whereas in the starbursting phase, high density gas clumps absorb $\sim 80\%$ of UV photons and re-emit the energy in infrared (IR) photons, thus the sub-millimeter flux increases. We find that the peak of SED shifts rapidly between UV and IR wavelengths on a time-scale of ~ 100 Myrs. We predict the detectability of high- z galaxies with the Atacama Large Millimeter Array (ALMA). For a sensitivity limit of 0.1 mJy (0.01 mJy) at 850 μm , the detection probability of galaxies in halos $M_{\text{h}} \gtrsim 10^{11} M_{\odot}$ ($M_{\text{h}} \gtrsim 10^{10.5} M_{\odot}$) at $z \lesssim 7$ ($z \lesssim 9$) exceeds 50%.

The Ly α luminosity and equivalent width (EW) also change with intermittent star formation. In starburst phase at $z > 10$, the maximum luminosity reaches $\sim 10^{41} \text{ erg s}^{-1}$ and $EW^{\text{Ly}\alpha} \gtrsim 30 \text{ \AA}$, thus such galaxies may be detected by JWST as a dust-free Ly α emitter. At $z < 10$, $\sim 90\%$ of Ly α photons are absorbed by dust, resulting in almost constant luminosity of $\sim 10^{41} - 10^{42} \text{ erg s}^{-1}$ and low EW even in starburst phase. The galactic size

increases with decreasing redshift, and becomes ~ 1 physical kpc at $z \sim 6$, which is consistent with observations (Kawamata *et al.* 2018). This compactness of high- z galaxies leads to stronger UV absorption by dust, resulting in high dust temperature.

References

- Bouwens, R. J., Illingworth, G. D., Oesch, P. A., Trenti, M., Labb  , I., Bradley, L., Carollo, M., van Dokkum, P. G., *et al.* 2015, *ApJ*, 803, 34
Hashimoto, T., Laporte, N., Mawatari, K., Ellis, R. S., Inoue, A. K., Zackrisson, E., Roberts-Borsani, G., Zheng, W., *et al.* 2018, *Nature*, 557, 392
Arata, S., Yajima, H., Nagamine, K., Li, Y., & Khochfar, S. 2018, [arXiv:1810.07621](https://arxiv.org/abs/1810.07621)
Yajima, H., Nagamine, K., Zhu, Q., Khochfar, S., & Dalla Vecchia, C. 2017, *ApJ*, 846, 30
Li, Y., Hopkins, P. F., Hernquist, L., Finkbeiner, D. P., Cox, T. J., Springel, V., Jiang, L., Fan, X., & Yoshida, N. 2008, *ApJ*, 678, 41
Yajima, H., Li, Y., Zhu, Q., & Abel, T. 2012, *MNRAS*, 424, 884
Kawamata, R., Ishigaki, M., Shimasaku, K., Oguri, M., Ouchi, M., & Tanigawa, S. 2018, *ApJ*, 855, 4